Molecular Spin Switch and Conversions of Localized Excess Electrons under External Electric Field: Solvated Dielectron $C_{20}F_{20}$@K@$C_{20}F_{20}$@K@$C_{20}F_{20}$

Jia-Min Tang [1], Yin-Feng Wang[1], Tian Qin[1], Xue-Xia Liu[1], Zhijun Wang[1], Jiangen Huang[1], Hua-Rong Zhang[1], Kai Yang[1], and Zhi-Ru Li[2]

[1]Jinggangshan University
[2]Jilin University

July 27, 2020

Abstract

By doping two potassium atoms among three $C_{20}F_{20}$ cages, peanut-shaped single molecular solvated dielectron $C_{20}F_{20}$@K@$C_{20}F_{20}$@K@$C_{20}F_{20}$ as new type of spin molecular switches was theoretically presented. The triplet structure with two single-excess-electrons individually inside left and middle cages is thermodynamically more stable than the singlet one with lone pair of excess electrons inside middle cage. It is found that applying an oriented external electric field (OEEF) of 111 × 10^{-4} au (0.5705 V/Å) or -120 × 10^{-4} au (-0.6168 V/Å) in the x-axis direction firstly and then releasing it, the field-free triplet $C_{20}F_{20}$@K@$C_{20}F_{20}$@K@$C_{20}F_{20}$ with two single-excess-electrons can change into singlet one with lone pair of excess electrons through a singlet one with lone pair of excess electrons inside the end cage. Different spin states can bring significantly different dipole moment component values and considerable different intensities of maxumum wavelengths in intense absorption band. Therefore, $C_{20}F_{20}$@K@$C_{20}F_{20}$@K@$C_{20}F_{20}$ is a good candidate for spin molecular switching materials.

Molecular Spin Switch and Conversions of Localized Excess Electrons under External Electric Field: Solvated Dielectron $C_{20}F_{20}$@K@$C_{20}F_{20}$@K@$C_{20}F_{20}$

Jia-Min Tang,[a] Yin-Feng Wang,*[a] Qin Tian,[a]Xue-Xia Liu,[a] Zhijun Wang,[a] Jiangen Huang,[a]Hua-Rong Zhang,*[b] Kai Yang,[a] and Zhi-Ru Li*[c]

[a] Dr. Y.-F. Wang, Bs. Q .Tian, Dr. X.-X. Liu, Dr. Z. Wang. Jiangxi Province Key Laboratory of Coordination Chemistry, School of Chemistry and Chemical Engineering, Jinggangshan University Ji'an, Jiangxi 343009 (P.R. China) E-mail: *cyclont@yeah.net*

[b] Dr. H.-R. Zhang Key Laboratory of Organosilicon Chemistry and Material Technology, Hangzhou Normal University, Hangzhou, Zhejiang 311121 (P.R. China). E-mail: *zhanghuaxy99@hznu.edu.cn*

[c] Prof. Z.-R. Li Institute of Theoretical Chemistry, Laboratory of Theoretical Computational Chemistry, Jilin University Changchun 130023 (P.R. China) E-mail: *lzr@jlu.edu.cn*

Abstract: By doping two potassium atoms among three $C_{20}F_{20}$ cages, peanut-shaped single molecular solvated dielectron $C_{20}F_{20}$@K@$C_{20}F_{20}$@K@$C_{20}F_{20}$as new type of spin molecular switches was theoretically presented. The triplet structure with two single-excess-electrons individually inside left and middle cages is thermodynamically more stable than the singlet one with lone pair of excess electrons inside middle cage. It is found that applying an oriented external electric field (OEEF) of 111 × 10^{-4} au (0.5705 V/Å) or -120 × 10^{-4}au (-0.6168 V/Å) in the x-axis direction firstly and then releasing it, the field-free triplet $C_{20}F_{20}$@K@$C_{20}F_{20}$@K@$C_{20}F_{20}$with two single-excess-electrons can change into singlet one with lone pair of

excess electrons through a singlet one with lone pair of excess electrons inside the end cage. Different spin states can bring significantly different dipole moment component values and considerable different intensities of maxumum wavelengths in intense absorption band. Therefore, $C_{20}F_{20}@K@C_{20}F_{20}@K@C_{20}F_{20}$is a good candidate for spin molecular switching materials.

Introduction

Recently, theoretical design of new high-performance molecular switching materials driven by oriented external electric field (OEEF) have witnessed large developments in the field of molecular electronics.[1-5]

As the simplest form of an extremely reactive intermediate, the investigation of the solvated electron plays a prominent role in physics, chemistry, and biochemistry.[6-14] For example, Adhikari et al have reported efficient capture of presolvated electrons by DNA base.[10] Also, for the charge- and electron-transfer and the transitions, manipulation of one or several electrons at the molecular level remains a highly challenging task[15] considering the utmost importance in the related fields of molecular electronics,[16] artificial photosynthesis,[15,17] molecular switches,[15,18] quantum-dot cellular automata (QCA),[19-21] solar cells,[22] and supramolecular assemblies.[23] As solvated electron systems (excess electron inside molecular cluster or cage) have not enough stabilities,[14] improving their stabilities is an important task.

To improve stabilities of general solvated electrons, in our recent series of papers,[24-29] basing on the synthesized $C_{20}F_{20}$ and potential $C_{24}F_{24}$ and $C_{60}F_{60}$ cage,[30,31] we have constructed a series of interesting cage-like single molecular solvated (di)electron systems with large stabilities due to the using covalent cages: $e@C_{60}F_{60}$, $e_2@C_nF_n$ (n=20, 28, 36, 50, 60, and 80), $e@C_{20}F_{18}(NH)_2C_{20}F_{18}$, and $e@C_{24}F_{22}(NH)_2C_{20}F_{18}$, which shows these perfluorinated cages are efficient containers of excess electrons. For these cages, the dipole moments of all the exo polarized $C^{\delta+}$-$F^{\delta-}$ bonds of each cage are directed toward the center of the cage to form an interior electronic attractive potential (IEAP) which can help to trap excess electron(s) inside these cages. These single molecular solvated (di)electron systems can provide a base of molecular electronics device. Basing on our $e@C_{20}F_{18}(NH)_2C_{20}F_{18}$, Ma et al., have successfully suggested a new type of molecular quantum-dot cellular automata (MQCA) candidate.[20,21]Recently, Li et al.,[32] have constructed new kind of electride molecular salts $e@C_{20}F_{19}(CH_2)_4NH_2\ldots Na^+$as novel, potential high-performance NLO materials. Also, basing on triple-cage-like electride salt $K^+[e@3C_8(O)]^-$, Li et al., also suggested[33] that multicage strategy is effective to enhance nonlinear optical (NLO) response. For the double-cage-like single molecular solvated single electron systems $e^-@C_{20}F_{18}(NH)_2C_{20}F_{18}$,[26-28]the excess electron can be trapped inside different cages to form interesting inter-cage electron transfer isomers.[26] In this case, besides the double-cage-like single molecular solvated electron systems,[20,21,26-28] We are interesting in the influence of the number of cage units on the localizations and spin states of two excess electrons. Especially, can it switch between different spin states by external stimulus? Obviously, exploring new molecular spin switching material is necessary for promoting its application in the field of molecular electronics, which is the target of our work.

Recently, Sadlej-Sosnowska has reported that, in an uniform OEEF, a reversible switching between the two configurations of Li-benzene complex with significant dipole moments took place.[34]Straka et al demonstrated for $MX@C_{70}$ (M: metal, X: nonmetal) systems that the relative orientation of enclosed MX with respect to a set of electrodes connected to the system can be controlled by application of OEEF(s).[2] For the double-cage-like single molecular solvated electron systems of $e@C_{20}F_{18}(NH)_2C_{20}F_{18}$, and $e@C_{24}F_{22}(NH)_2C_{20}F_{18}$,[26-27]we have also used an external electric field to realize the inter-cage excess electron transfer and isomerization among three inter-cage electron transfer isomers. These will provide an approach for the manipulating localization(s) and spin states of the excess electron(s) in multi-cage-shaped solvated dielectron systems by using external electric field.

In this paper, by doping two potassium atoms among three $C_{20}F_{20}$ cages, our investigation aims at obtaining the structures, excess electron localizations, and electronic absorption spectra of the peanut-shaped single molecular solvated dielectron systems of $C_{20}F_{20}@K@C_{20}F_{20}@K@C_{20}F_{20}$, revealing the influence of the number of cage units on the localizations and spin states of two excess electrons, exhibiting excess electron transition under the external electric field, and suggesting the possible candidate for the new kind of

molecular spin switching metherial.

Results and Discussion

Geometrical characteristics and excess electron localizations

The optimized geometries with all real frequencies of $C_{20}F_{20}$@K@$C_{20}F_{20}$@K@$C_{20}F_{20}$were shown in Figure 1. The selected structural parameters in both singlet and triplet states were listed in Table 1. For both singlet (S) and triplet structures (T), the $C_{20}F_{20}$@K@$C_{20}F_{20}$@K@$C_{20}F_{20}$represents face-to-face stacked $C_{20}F_{20}$cages connected by two doped K atoms. From Figure 1, for the plane where five-membered ring is located, the plane α of cage **1** and plane β of cage **2** are staggered with very small dihedral angle (0.55 (S) or 0.26°(T)). The similar situation happens between the five-membered plane γ (cage **2**) and δ (cage**3**) but some large dihedral angle between them (15.08 (S) or 15.55°(T)).

The different sizes of three cages (**1** , **2** , and**3**) are closely related to excess electron localization(s) in both states (S and T). Results in Table 1 exhibit that cage **2**are the smallest one among three cages (h_2(**2**) < h_1 (**1**) [?]h_3 (**3**)) in singlet structure, and both cage **2** (h_2) and **1**(h_1) are smaller in size than cage **3**(h_3) in triplet one.

Results in Table 2 show that the natural popular analysis (NPA) charges of K1 and K2 atoms in field-free $C_{20}F_{20}$@K@$C_{20}F_{20}$@K@$C_{20}F_{20}$are larger than 0.66 |e| for both singlet and triplet states, which indicates the valences of both K atoms are +1 for both states. At the same time, the NPA charge of cage **2** in singlet structure and that of cage **1** and **2** in triplet one suggests that the valence of cage **2** in singlet structure is -2 and that of both cage **1** and **2** are -1. Therefore, the 4s electrons of both K atoms are pulled out and trapped inside the fluorinated C_{20} cage(s) to form localized excess electrons due to the IEAPs.

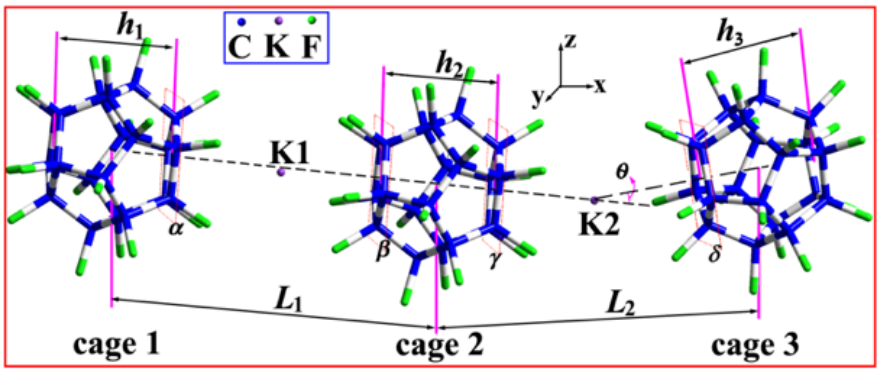

Figure 1. Optimized geometries of $C_{20}F_{20}$@K@$C_{20}F_{20}$@K@$C_{20}F_{20}$.

Table 1. Selected mean structural parameters of field-free $C_{20}F_{20}$@K@$C_{20}F_{20}$@K@$C_{20}F_{20}$.

	$C_{20}F_{20}$@K@$C_{20}F_{20}$@K@$C_{20}F_{20}$	$C_{20}F_{20}$@K@$C_{20}F_{20}$@K@$C_{20}F_{20}$
	Singlet state (S)	Triplet state (T)
h_1 (Å)	3.444	3.415
h_2 (Å)	3.375	3.402
h_3 (Å)	3.445	3.447
L_1 (Å)	9.583	9.577
L_2 (Å)	9.505	9.569
ϑ (°)	8.25	8.32
α & β (°)[a]	0.55	0.26
γ & δ (°)[a]	15.08	15.55

[a] Dihedral angle

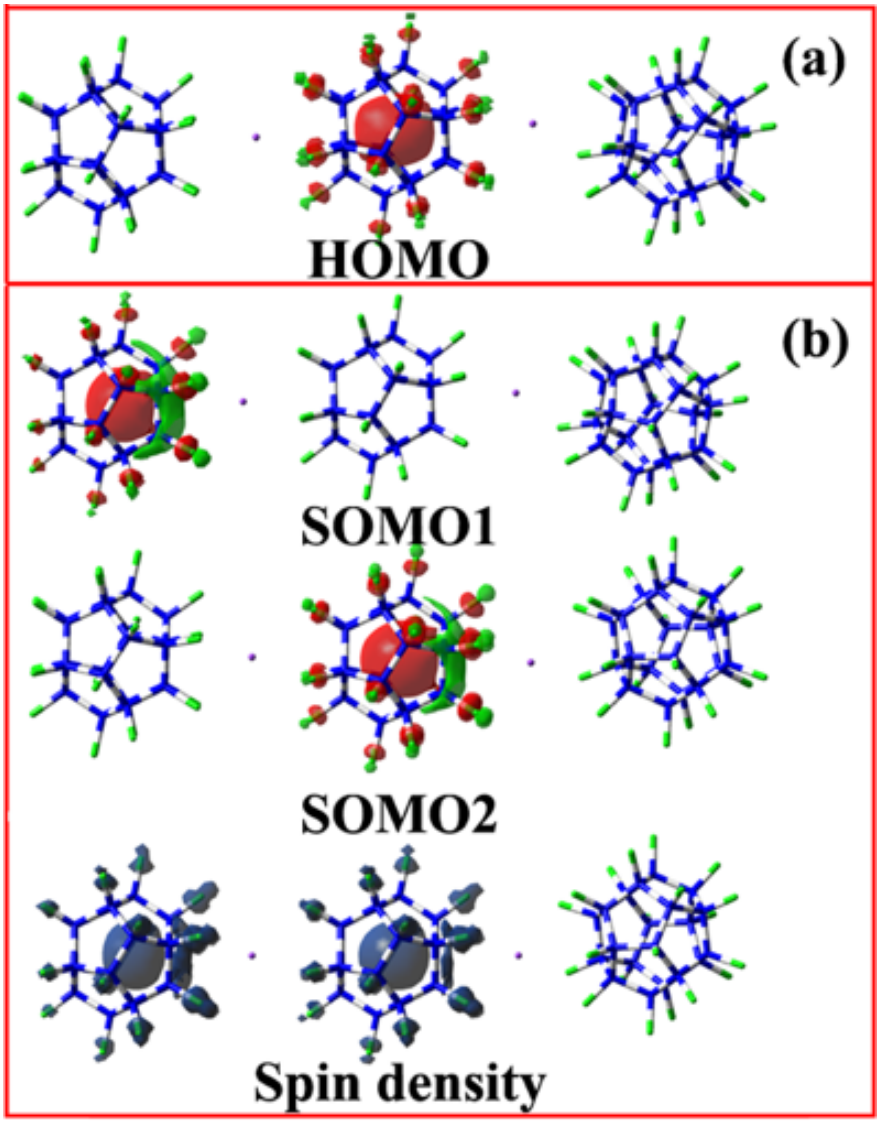

Figure 2. Selected frontier molecular orbitals (isovalue of 0.04 au) in both states, spin density distribution (isovalue of 0.004 au) in triplet $C_{20}F_{20}$@K@$C_{20}F_{20}$@K@$C_{20}F_{20}$. a) singlet and b) triplet state.

Table 2. Natural popular analysis (NPA, |e|) charge and Dipole moments (μ_ξ. Δ) of $C_{20}F_{20}$@K@$C_{20}F_{20}$@K@$C_{20}F_{20}$under different external electric fields (*EEFs*).

	$C_{20}F_{20}$@K@$C_{20}F_{20}$@K@$C_{20}F_{20}$	$C_{20}F_{20}$@K@$C_{20}F_{20}$@K@$C_{20}F_{20}$
	Singlet state (S)	Triplet state (T)
F_x = -120 × 10 $^{-4}$ au	F_x = -120 × 10 $^{-4}$ au	F_x = -120 × 10 $^{-4}$ au
K1	0.710	0.708
K2	0.651	0.662
Cage **1**	0.157	0.165
Cage **2**	0.169	-0.636

	$C_{20}F_{20}$@K@$C_{20}F_{20}$@K@$C_{20}F_{20}$	$C_{20}F_{20}$@K@$C_{20}F_{20}$@K@$C_{20}F_{20}$
Cage **3**	-1.687	-0.899
μ_ξ	98.77	104.96
F_x = -20 × 10 $^{-4}$ au	F_x = -20 × 10 $^{-4}$ au	F_x = -20 × 10 $^{-4}$ au
K1	0.690	0.701
K2	0.646	0.687
Cage **1**	0.129	0.146
Cage **2**	-1.172	-0.692
Cage **3**	-0.294	-0.842
μ_ξ	22.16	48.26
F_x = 0 au	F_x = 0 au	F_x = 0 au
K1	0.664	0.678
K2	0.667	0.703
Cage **1**	0.007	-0.816
Cage **2**	-1.345	-0.688
Cage **3**	0.006	0.122
μ_ξ	0.03	-35.20
F_x = 111 × 10 $^{-4}$ au	F_x = 111 × 10 $^{-4}$ au	F_x = 111 × 10 $^{-4}$ au
K1	0.645	0.833
K2	0.713	0.890
Cage **1**	-1.592	-1.173
Cage **2**	0.081	-0.612
Cage **3**	0.153	0.063
μ_ξ	-98.78	-97.99

Figure 2 gives the frontier molecular orbitals in both states and spin density distribution in triplet state. The highest occupied molecular orbital (HOMO, see Figure 2a) in singlet state indicates that two excess electrons are trapped inside the middle smallest-sized $C_{20}F_{20}$ cage (**2**) with NPA charge of -1.345 |e| to form a lone pair of excess electrons. From Figure 2b, the two single occupied molecular orbitals (SOMO1 and SOMO2) and spin density distribution suggest one excess electron is confined inside the left $C_{20}F_{20}$ cage (**1**) with NPA charge of -0.816 |e| and the other one is confined inside the middle $C_{20}F_{20}$ cage (**2**) with NPA charge of -0.688 |e|. Then, the two excess electrons are two single-excess-electrons individually inside left (**1**) and middle cage **2** . The right largest-sized $C_{20}F_{20}$ cage (**3**) is empty for triplet $C_{20}F_{20}$@K@$C_{20}F_{20}$@K@$C_{20}F_{20}$. The sizes of the occupied $C_{20}F_{20}$ cage(s) are slightly smaller than that of the unoccupied one for both states, which shows that the occupation of electrons makes the occupied cage slightly shrink. These are similar to that of the reported e@$C_{20}F_{18}(NH)_2C_{20}F_{18}$and e@$C_{24}F_{22}(NH)_2C_{20}F_{18}$.[26,27]

Therefore, the lone pair of excess electrons is confined inside the middle smallest-sized $C_{20}F_{20}$ cage (**2**) for singlet $C_{20}F_{20}$@K@$C_{20}F_{20}$@K@$C_{20}F_{20}$, while two single-excess-electrons are, respectively, confined inside left and middle smaller-sized $C_{20}F_{20}$cages (**1** and **2**) for triplet $C_{20}F_{20}$@K@$C_{20}F_{20}$@K@$C_{20}F_{20}$.

Of course, different spatial localizations of the excess electrons lead to clearly different physical properties. From Table 2), the dipole moment component μ_x values are, respectively, 0.03 and -35.2 D for singlet structure with lone pair of excess electrons inside smallest-sized $C_{20}F_{20}$cage (**2**) and triplet one with two single-excess electrons inside left and middle small-sized $C_{20}F_{20}$ cages (**1** and**2**). The difference of μ_ξ values between singlet and triplet states is much considerable.

It is reported that, for e@$C_{20}F_{18}(NH)_2C_{20}F_{18}$,[26]there exists a third structure with an excess electron equally confined in both $C_{20}F_{18}$ cages. Similarly, a triplet structure with D_{5d} point group of $C_{20}F_{20}$@K@$C_{20}F_{20}$@K@$C_{20}F_{20}$has been found during our searching. This tripletD_{5d} structure shows that one excess electron is confined inside the middle $C_{20}F_{20}$ cage (**2**), and the other one is equally confined

in both end $C_{20}F_{20}$ cage (**1** and **3)** . However, this D_{5d} structure is a transition state due to five large imaginary frequencies.

Evolution of excess electron localizations

Recently, we have reported that application of OEEF of -10 × 10^{-4} au (-0.0514 V/Å) results in of an excess electron transfer from left to right cage of $e@C_{20}F_{18}(NH)_2C_{20}F_{18}$.[27]For singlet and triplet $C_{20}F_{20}@K@C_{20}F_{20}@K@C_{20}F_{20}$, the conversions of two excess electrons in three $C_{20}F_{20}$ cages are especially deserved studied. Both Figure 3 and Table 2 give the evolutions of NPA charges of three cages (**1** , **2** , and **3**) under OEEFs.

For singlet $C_{20}F_{20}@K@C_{20}F_{20}@K@C_{20}F_{20}$, one can see that the absolute value of NPA charge of cage **2**decreases with increasing the intensity of OEEF in both positive and negative directions of x-axis (from F_x = 0 to 125 or -125 × 10^{-4} au). Simultaneously, the absolute value of NPA charge of cage **1** increases but that of cage **3**decrease as changing the intensity of OEEF in x-axis direction fromF_x = -125 × 10^{-4} to 125 × 10^{-4} au. The NPA charge of cage **1** underF_x = 111 × 10^{-4} au (0.5705 V/Å) and that of cage **3** under F_x = -120 × 10^{-4} au (0.6168 V/Å) in singlet $C_{20}F_{20}@K@C_{20}F_{20}@K@C_{20}F_{20}$are, respectively, -1.592 |e| and -1.687 |e|. The HOMOs of singlet $C_{20}F_{20}@K@C_{20}F_{20}@K@C_{20}F_{20}$with and without F_x are also shown in Figure 3a. From the analysis of HOMOs in Figure 3a, the lone pair of excess electrons is confined inside the left $C_{20}F_{20}$ cage (**1**) for $C_{20}F_{20}@K@C_{20}F_{20}@K@C_{20}F_{20}$under F_x = 111 × 10^{-4} au (0.5705 V/Å) and that is confined inside the right one (**3**) for $C_{20}F_{20}@K@C_{20}F_{20}@K@C_{20}F_{20}$under F_x = -120 × 10^{-4} au (-0.6168 V/Å). Therefore, applying the OEEF of 111 × 10^{-4} au (0.5705 V/Å) and -120 × 10^{-4}au (-0.6168 V/Å) in the x-axis direction of singlet $C_{20}F_{20}@K@C_{20}F_{20}@K@C_{20}F_{20}$results in the transfer of the lone pair of excess electrons from middle $C_{20}F_{20}$ cage (**2**) to left $C_{20}F_{20}$ cage (**1**) and from middle $C_{20}F_{20}$ cage (**2**) to right $C_{20}F_{20}$ cage (**3**), respectively. The μ_ξ value increases enormously when going from field-free singlet $C_{20}F_{20}@K@C_{20}F_{20}@K@C_{20}F_2$with lone pair of excess electrons inside middle $C_{20}F_{20}$ cage (**2**) to the electrified ones with that inside end $C_{20}F_{20}$ cage (**1** or **3**).

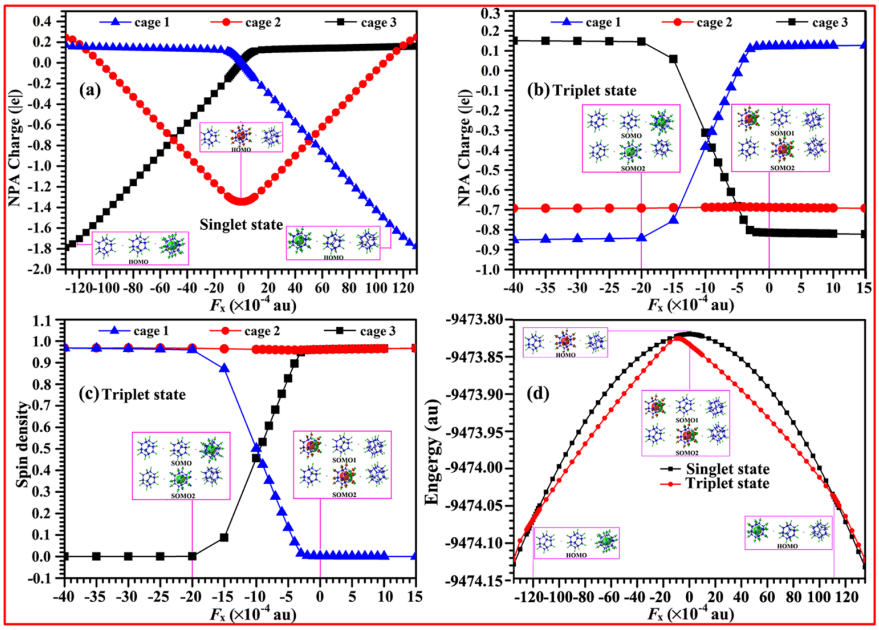

Figure 3. a) Evolution of NPA charges in singlet state, b) evolution of NPA charges in triplet state, c) evolution of spin density in triplet state, and d) evolution of energy under external electric fields (EEFs). molecular orbitals at the isovalue of 0.004 au.

For triplet $C_{20}F_{20}$@K@$C_{20}F_{20}$@K@$C_{20}F_{20}$, from Figure 3b and Table 2 as well as Figure 3c, it can be found that both spin density and the absolute values of NPA charges of cage**1** decrease but that of cage **3** increase with increasing the intensity of OEEF in negative directions of x-axis (from$F_x = 0$ to -40 × 10^{-4} au). The NPA charge of cage **1** under $F_x = 0$ au and that of cage **3** under F_x = -20 × 10^{-4} au (-0.1018 V/Å) in triplet $C_{20}F_{20}$@K@$C_{20}F_{20}$@K@$C_{20}F_{20}$are, respectively, -0.816 |e| and -0.842 |e|. The SOMOs show that an excess electron is confined inside the left $C_{20}F_{20}$ cage (**1**) for $C_{20}F_{20}$@K@$C_{20}F_{20}$@K@$C_{20}F_{20}$under F_x = 0 au but that is confined inside the right $C_{20}F_{20}$ cage (**3**) for $C_{20}F_{20}$@K@$C_{20}F_{20}$@K@$C_{20}F_{20}$under F_x = -20 × 10^{-4} au (-0.1018 V/Å).

Therefore, applying an OEEF of -20 × 10^{-4} au (-0.1018 V/Å) in the x-axis direction of triplet $C_{20}F_{20}$@K@$C_{20}F_{20}$@K@$C_{20}F_{20}$results in both left-to-right transfers of the two single-excess-electrons. The transfers of the excess electrons are exhibited that a single-excess-electron transfers from middle $C_{20}F_{20}$ cage (**2**) to right $C_{20}F_{20}$ cage (**3**) and the other one transfers from right cage (**1**) to middle $C_{20}F_{20}$ cage (**2**). Theμ_ξ value also increases enormously when going from field-free triplet $C_{20}F_{20}$@K@$C_{20}F_{20}$@K@$C_{20}F_2$to electrified ones.

Molecular spin switch and stabilities

By comparing the total energies for field-free $C_{20}F_{20}$@K@$C_{20}F_{20}$@K@$C_{20}F_{20}$in different spin states (see Table 3), it is found that the triplet structure is 8.72 kcal/mol in energy lower than the corresponding singlet one. Therefore, owing to different localizations of the excess electrons, the triplet structure with two single-excess-electrons inside two cages (**1** and **2**) is thermodynamically more stable than the singlet one with lone pair of excess electrons inside one cage (**2**) for field-free $C_{20}F_{20}$@K@$C_{20}F_{20}$@K@$C_{20}F_{20}$. So, the triplet structure is the ground state for field-free $C_{20}F_{20}$@K@$C_{20}F_{20}$@K@$C_{20}F_{20}$. In addition, the small energy difference between singlet and triplet structures may be beneficial to the interconversion between them.

It is worth noticing that, results in Figure 3d and Table 3 show that the energies of triplet $C_{20}F_{20}$@K@$C_{20}F_{20}$@K@$C_{20}F_{20}$under both F_x < 111 × 10^{-4} and F_x > -120 × 10^{-4} au are lower than that of singlet one, while the singlet $C_{20}F_{20}$@K@$C_{20}F_{20}$@K@$C_{20}F_{20}$under both F_x [?] 111 x 10^{-4} andF_x [?] -120 x 10^{-4} au are lower in energy than the triplet one. That is to say, the triplet $C_{20}F_{20}$@K@$C_{20}F_{20}$@K@$C_{20}F_{20}$with the range of -120 x 10^{-4} <F_x < 111 x 10^{-4} au but singlet one with the range of F_x [?] 111 x 10^{-4} or [?] -120 x 10^{-4} au are ground state for $C_{20}F_{20}$@K@$C_{20}F_{20}$@K@$C_{20}F_{20}$.

Considering the electronic stabilities of $C_{20}F_{20}$@K@$C_{20}F_{20}$@K@$C_{20}F_{20}$, we focus on the first and second vertical electron detachment energies (VDE (I) and (II)) in ground state. From Table 3, for the triplet $C_{20}F_{20}$@K@$C_{20}F_{20}$@K@$C_{20}F_{20}$, the VDE (I) and VDE(II) values are 6.61 and 9.34 eV, respectively. These VDEs are far larger than that of the reported solvated dielectron e_2@$C_{60}F_{60}$ structures ((VDEs (I) of 1.720 ˜ 2.283 eV, and VDEs (II) of 3.959–5.288 eV)),[25]e_2@$(LiF)_n$ (n = 3 ˜ 5, -0.021 ˜ 1.254 eV (VDE(1))),[35] and dipole bound dianions of [$(PF_5)_3$***dropentalene - Ca].[36] Obviously, the triplet $C_{20}F_{20}$@K@$C_{20}F_{20}$@K@$C_{20}F_{20}$are stable solvated dielectrons. Changing from triplet to singlet $C_{20}F_{20}$@K@$C_{20}F_{20}$@K@$C_{20}F_{20}$, both VDE (I) and VDE(II) values considerably decrease to 4.42 and 8.33 eV as applying the *EEF* of -120 x 10^{-4} au in the x-axis direction but significantly increase to 11.56 and 13.14 eV as applying the *EEF* of 110 x 10^{-4} au in the x-axis direction. Still, the VDE (I) and VDE(II) values singlet $C_{20}F_{20}$@K@$C_{20}F_{20}$@K@$C_{20}F_{20}$under F_x = -120 x 10^{-4} au are far larger than the corresponding ones of reported e_2@$C_{60}F_{60}$ and e_2@$(LiF)_n$, which indicates that the singlet $C_{20}F_{20}$@K@$C_{20}F_{20}$@K@$C_{20}F_{20}$under F_x = 111 x 10^{-4} or -120 x 10^{-4} au may be still stable.

Table 3. Total energies (E_{tot}, au), relative energies (E_{rel}, kcal/mol), interaction energies (E_{int}), and vertical detachment energies (VDE(I&II), eV).

	$C_{20}F_{20}$@K@$C_{20}F_{20}$@K@$C_{20}F_{20}$	$C_{20}F_{20}$@K@$C_{20}F_{20}$@K@$C_{20}F_{20}$
	Singlet state (S)	Triplet state (T)
F_x = -120 × 10^{-4} au	F_x = -120 × 10^{-4} au	F_x = -120 × 10^{-4} au
E_{tot}	-9474.070590	-9474.070150

	$C_{20}F_{20}$@K@$C_{20}F_{20}$@K@$C_{20}F_{20}$	$C_{20}F_{20}$@K@$C_{20}F_{20}$@K@$C_{20}F_{20}$
E_{rel}	0.00	0.28
VDE(I)	4.42	
VDE(II)	8.33	
$F_x = 0$ au	$F_x = 0$ au	$F_x = 0$ au
E_{tot}	-9473.818630	-9473.832540
E_{rel}	0.00	-8.72
VDE(I)		6.61
VDE(II)		9.34
$F_x = 111 \times 10^{-4}$ au	$F_x = 111 \times 10^{-4}$ au	$F_x = 111 \times 10^{-4}$ au
E_{tot}	-9747.039340	-0.9747.038810
E_{rel}	0.00	0.33
VDE(I)	11.56	97
VDE(II)	13.14	

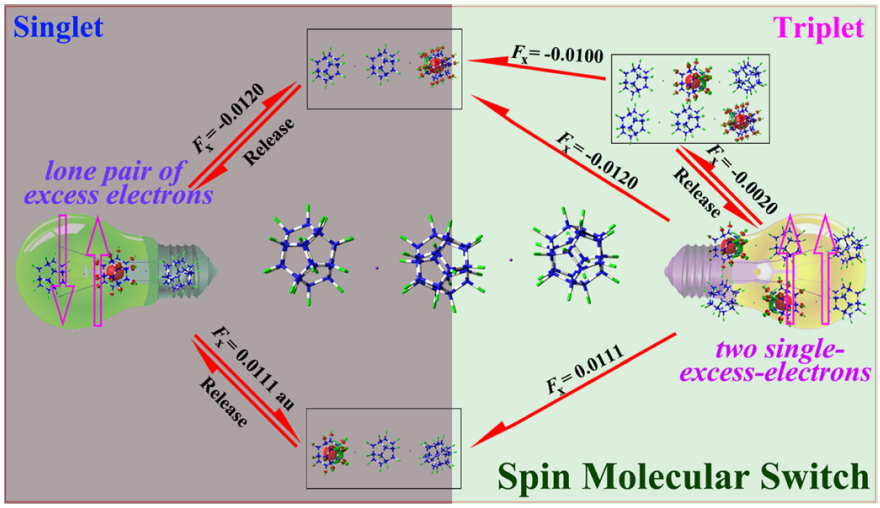

Figure 4. Diagram of spin switching character of $C_{20}F_{20}$@K@$C_{20}F_{20}$@K@$C_{20}F_{20}$.

Therefore, applying an OEEF of 111 × 10^{-4} or -120 × 10^{-4} au in the x-axis direction of field-free triplet $C_{20}F_{20}$@K@$C_{20}F_{20}$@K@$C_{20}F_{20}$can reduce two single-excess-electrons (triplet state) moving to the end-one (**1** or **3**) and changing into lone pair of excess electrons (singlet state). Subsequently, the field-free triplet $C_{20}F_{20}$@K@$C_{20}F_{20}$@K@$C_{20}F_{20}$changing into electrified singlet one. And then, releasing the OEEF can result in the movement of lone pair of excess electrons from end cage (**1** or **3**) to middle one (**2** , see Figure 4) and the electrified singlet $C_{20}F_{20}$@K@$C_{20}F_{20}$@K@$C_{20}F_{20}$with lone pair of excess electrons inside end cage (**1** or**3**) changing into field-free singlet one with that inside middle cage (**2**). That is to say, applying a suitable OEEF firstly and then releasing it, the field-free triplet $C_{20}F_{20}$@K@$C_{20}F_{20}$@K@$C_{20}F_{20}$with two single-excess-electrons individually inside left cage (**1**) and middle cage (**2**) can change into singlet $C_{20}F_{20}$@K@$C_{20}F_{20}$@K@$C_{20}F_{20}$with lone pair of excess electrons inside middle cage (**2**).

Electronic Absorption Spectra

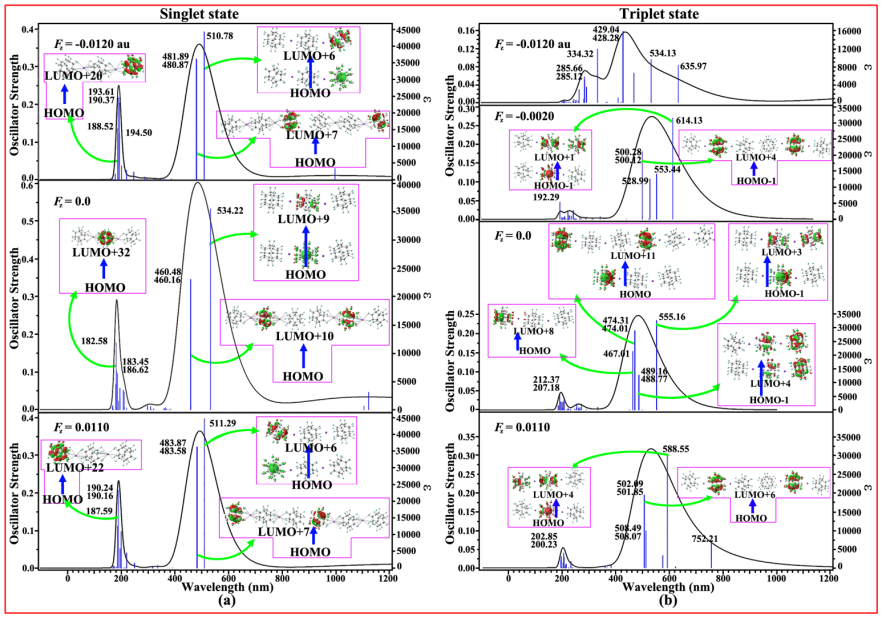

Figure 5. Excess electronic absorption spectra at CIS/6-31G (d) level, a) singlet state and b) triplet state.

The electronic absorption spectra of the $C_{20}F_{20}$@K@$C_{20}F_{20}$@K@$C_{20}F_{20}$with and without OEEFs are depicted in Figure 5. The diagram of these selected electronic excitations and the contour plots for their corresponding molecular orbitals (MOs) are also presented in Figure 5.

From Figure 5a, it shows an intense absorption band with two maximum absorption (wavelengths of 534 and 460 nm) and a weaker absorption band at 183 nm for the field-free singlet $C_{20}F_{20}$@K@$C_{20}F_{20}$@K@$C_{20}F_{20}$with the lone pair of excess electrons inside middle $C_{20}F_{20}$ cage (**2**). When going from field-free $C_{20}F_{20}$@K@$C_{20}F_{20}$@K@$C_{20}F_2$with lone pair of excess electrons inside middle $C_{20}F_{20}$ cage (**2**) to the electrified ones with that inside the left or right $C_{20}F_{20}$ cage (**1** or **3**), it is found that the absorption in long wavelength appears blue-shift (from 534 to 511 nm) and that on short wavelengths appear red-shift (from 460 to 481 or 484 nm) for the intense absorption band. The two absorption bands of $C_{20}F_{20}$@K@$C_{20}F_{20}$@K@$C_{20}F_{20}$under $F_x = -120 \times 10^{-4}$ au with lone pair of excess electrons inside the right $C_{20}F_{20}$ cage (**3**) are almost same to that under $F_x = 110 \times 10^{-4}$au with that inside the left $C_{20}F_{20}$ cage (**1**). Results in Fig. 5a also shows that the electronic excitation of each above absorption bands corresponds to intra-cage s - p transition for all three $C_{20}F_{20}$@K@$C_{20}F_{20}$@K@$C_{20}F_{20}$under $F_x = -120 \times 10^{-4}$, 0 and 120×10^{-4} au with lone pair of excess electrons inside right, middle and left cage, respectively.

From Figure 5b, it shows an intense absorption band with three maximum absorptions (wavelengths of 555, 474, and 467 nm) and a much weaker absorption band at 212 nm for field-free triplet $C_{20}F_{20}$@K@$C_{20}F_{20}$@K@$C_{20}F_{20}$with two single-excess-electrons, respectively, inside the left and middle $C_{20}F_{20}$ cages (**1** and**2**). The electronic excitation of the strongest absorption (555 nm) corresponds to intra- and inter-cage s - p transitions (HOMO-1 - LUMO+3), while that of the second and third ones (474 and 467 nm) corresponds to intra-cage s - p transitions (HOMO - LUMO+11 and LUMO+8). Obviously, the intense absorption bands with absorption wavelengths of 555 and 474 nm for field-free triplet $C_{20}F_{20}$@K@$C_{20}F_{20}$@K@$C_{20}F_{20}$with two single-excess-electrons inside two cages (**1** and**2**) just corresponds to that of 534 and 460 nm for field-free singlet $C_{20}F_{20}$@K@$C_{20}F_{20}$@K@$C_{20}F_{20}$with the lone pair of excess electrons inside one cage (**2**), respectively. From field-free triplet to field-free singlet $C_{20}F_{20}$@K@$C_{20}F_{20}$@K@$C_{20}F_{20}$, the wavelengths of both absorptions appear blue-shift and intensity of both absorptions considerably strengthen. When going from field-free triplet $C_{20}F_{20}$@K@$C_{20}F_{20}$@K@$C_{20}F_2$with two single-excess-electrons inside left and middle $C_{20}F_{20}$ cage (**1** and **2**) to the electrified ones with that

inside the middle or right $C_{20}F_{20}$ cage (**2** and **3**), it is found that the absorption in long wavelengths appears both red-shifts for the intense absorption band.

Conclusion

In this paper, we have presented a new kind of spin molecular switches by doping two potassium atoms among three $C_{20}F_{20}$ cages to form peanut-shaped single molecular solvated dielectron $C_{20}F_{20}$@K@$C_{20}F_{20}$@K@$C_{20}F_{20}$.

The triplet structure with two single-excess-electrons inside two cages (**1** and **2**) is thermodynamically more stable than the singlet one with lone pair of excess electrons inside one cage (**2**) for field-free $C_{20}F_{20}$@K@$C_{20}F_{20}$@K@$C_{20}F_{20}$.

For the localizations of excess electrons, it is found that the lone pair of excess electrons moves from middle $C_{20}F_{20}$ cage to right or left one by applying an OEEF of 111 x 10^{-4} au (0.5705 V/A) or -120 x 10^{-4} au (-0.6168 V/A) in the x-axis direction of singlet $C_{20}F_{20}$@K@$C_{20}F_{20}$@K@$C_{20}F_{20}$. Applying an OEEF of -20 x 10^{-4} au (-0.1018 V/A) in the x-axis direction of triplet $C_{20}F_{20}$@K@$C_{20}F_{20}$@K@$C_{20}F_{20}$can result in both left-to-right transfers of the two single-excess-electrons.

For the interconversion between spin states, it is found that applying an OEEF of 111 x 10^{-4} or -120 x 10^{-4}au in the x-axis direction of triplet $C_{20}F_{20}$@K@$C_{20}F_{20}$@K@$C_{20}F_{20}$firstly and then releasing it can reduce two single-excess-electron (triplet state) changing into lone pair of excess electrons (singlet state) and triplet $C_{20}F_{20}$@K@$C_{20}F_{20}$@K@$C_{20}F_{20}$changing into singlet one. the field-free triplet $C_{20}F_{20}$@K@$C_{20}F_{20}$@K@$C_{20}F_{20}$with two Different spin states can bring significantly different dipole moment component values and considerable different intensities of maxumum wavelengths in intense absorption band.

Therefore, $C_{20}F_{20}$@K@$C_{20}F_{20}$@K@$C_{20}F_{20}$is a good candidate for spin molecular switching material.

Computational Details

Because of our research systems including long-range interaction and charge transfer, the density functional, coulomb-attenuated hybrid exchange-correlation functional (CAM-B3LYP),[37] is used. It was reported that CAM-B3LYP provides molecular geometries close to experimentally observed structures.[38] In this work, the optimized geometric structures of the $C_{20}F_{20}$@K@$C_{20}F_{20}$@K@$C_{20}F_{20}$with all real frequencies in both singlet and triplet states are obtained at CAM-B3LYP/6-31G(d) level. The spin density distribution and natural popular analysis (NPA)[39] of the structures were also obtained at CAM-B3LYP/6-31G(d) level.

Recently, Population and novel hybrid meta exchange-correlation functional M06-2X[40] were successfully used to calculate the vertical electron detachment energy (VDE) of series of excess electron systems.[4,5, 41,42] Therefore, the VDEs of our structures were calculated at M06-2X/6-31G(2d) level, as the following formulas (Cage = $C_{20}F_{20}$@K@$C_{20}F_{20}$@K@$C_{20}F_{20}$):

VDE (I) = E $[Cage]^{+}_{opt}$ -E $[Cage]_{opt}$ (1)

VDE (II) = E $[Cage]^{2+}_{opt}$ -E $[Cage]^{+}_{opt}$ (2)

The spin contamination is negligible. In the calculations, the expected values of spin eigenvalue ¡S^{2}¿ are 0.0 for [Cage] (singlet) and 2.0 for M^{2+} (triplet), 0.75 for $[Cage]^{+}$, and 0.0 for $[Cage]^{2+}$ species.

In our previous work,[28] it is found that the first transition energy of CIS method is more close to the higher SAC-CI results than the TD-HF, TD-B3LYP, TD-CAM-B3LYP and TD-LC-BLYP results for molecular cluster anion $(FH)_2\{e^{-}\}(FH)$ and neutral (HCN)***Li with excess electron. Therefore, The CIS/6-31G(d) calculations were performed to obtain the excess electronic absorption spectrum of the $C_{20}F_{20}$@K@$C_{20}F_{20}$@K@$C_{20}F_{20}$.

The calculations were performed with the GAUSSIAN program package (GAUSSIAN 09 A02).[43]

Acknowledgements

We acknowledge the financial support from the National Natural Science Foundation of China (Nos. 21662018, and 21764007). This work was also supported by the Science and Technology Project of Jiangxi Provincial Department of Science &Technology (No. 20192BAB203005), and the Natural Science Foundation of Zhejiang Province (No. LQ17E030001).

Keywords: Spin switch * solvated electron* external electric field * electron localization * DFT

1. S. Shaik, R. Ramanan, D. Danovich, D. Mandal, *Chem. Soc. Rev* ,**2018** , *47* , 5125-5145.
2. A. Jaroš, E. F. Bonab, M. Straka, C. Foroutan-Nejad, *J. Am. Chem. Soc* , **2019** , *141* , 19644-19654.
3. A. A. Arabi, C.F. Matta, *J. Phys. Chem. B* , **2018** ,*122* , 8631-8641.
4. Y.-F. Wang, J. Li, J. Huang, T. Qin, Y.-M. Liu, F. Zhong, W. Zhang, Z.-R. Li, *J. Phys. Chem. C,* **2019** , *123* , 23610-23619.
5. J.-J. Wang, Z.-J. Zhou, H.-M. He, D. Wu, Y. Li, Z.-R. Li, H.-X. Zhang,*J. Phys. Chem. C,* **2016** , *120* , 13656-13666.
6. R. M. Young, D. M. Neumark, *Chem. Rev* , **2012** ,*112* , 5553-5577.
7. C. Zhang, Q. Luo, S. Cheng, Y. Bu, *J. Phys. Chem. Lett,***2018** , *9* , 689-695.
8. L. Mones, G. Pohlb, L, Turi, *Phys. Chem. Chem. Phys* ,**2018** , *20* , 28741-28750.
9. M. Mauksch, S. B. Tsogoeva, *Phys. Chem. Chem. Phys* ,**2018** , *20* , 27740-27744.
10. L. Das, S. Adhikari, *J. Phys. Chem. B,* **2018** ,*122* , 8900-8907.
11. A. H. C. West, B. L. Yoder, D. Luckhaus, C. Saak, M. Doppelbauer, R. Signorell, *J. Phys. Chem. Lett,* **2015** , *6* , 1487-1492.
12. S. H. Lin, M. Fujitsuka, T, Majima, T. *Chem. Eur. J,***2015** , *21* , 16190-16194.
13. B. Abel, U. Buck, A. L. Sobolewskic, W. Domcke, *Phys. Chem. Chem. Phys* , **2012** , *14* , 22-34.
14. J. Simons, *J. Phys. Chem. A* , **2008** , *112* , 6401-6511.
15. J. Fortage, C. Peltier, C. Perruchot, Y. Takemoto, Y. Teki, F. Bedioui, V. Marvaud, G. Dupeyre, L. Pospísil, C. Adamo, M. Hromadova, I. Ciofini, P. P. Laine, *J. Am. Chem. Soc* , **2012** ,*134* , 2691-2705.
16. Joachim, J. K. Gimzewski, A. Aviram, *Nature* , **2000** , 408, 541-548.
17. L. L. Tinker, N. D. McDaniel, S. Bernhard, *J. Mater. Chem* ,**2009** , 19, 3328-3337.
18. D. L. Ma, C. M. Che, S. C. Yan, *J. Am. Chem. Soc* ,**2009** , *131* , 1835-1846.
19. I. Amlani, A. O. Orlov, G. Toth, G. H. Bernstein, C. S. Lent, G. L. Snider, *Science* , **1999** , *284* , 289-291.
20. X. Wang, J. Ma, *Phys. Chem. Chem. Phys* , **2011** ,*13* , 16134-16137.
21. X. Wang, S. Chen, J. Wen, J. Ma, *J. Phys. Chem. C* ,**2013** , *117* , 1308-1314.
22. S. Ito, H. Miura, S. Uchida, M. Takata, K. Sumioka, P. Liska, P. Comte, P. Pechy, M. Graetzel, *Chem. Commun* , **2008** , 5194-5194.
23. K. Senechal-David, A. Hemeryck, N. Tancrez, L. Toupet, J. A. G. Williams, I. Ledoux, J. Zyss, A. Boucekkine, J. P. Guegan, H. Le Bozec, O. Maury, *J. Am. Chem. Soc* , **2006** , *128* , 12243-12255.
24. Y.-F. Wang, Z.-R. Li, D. Wu, C.-C. Sun, F.-L. Gu, *J. Comput. Chem* , **2010** , *31* , 195-203.
25. Y.-F. Wang, W. Chen, G.-T. Yu, Z.-R. Li, D. Wu, C.-C. Sun, *J. Comput. Chem* , **2011** , *32* , 2012-2021.
26. Y.-F. Wang, Y. Li, Z.-J. Zhou, Z.-R. Li, D. Wu, J. Huang, F. L. Gu,*ChemPhysChem* , **2012** , *13* , 756-761.
27. Y.-F. Wang, J. Huang, G. Zhou, Z.-R. Li, *Acta. Phys-Chim. Sin. B* , **2012** , *28* , 2574-2580.
28. Y.-F. Wang, Z.-R. Li, D. Wu, Y. Li, C.-C. Sun, F L. Gu, *J. Phys. Chem. A* , **2010** , *114* , 11782-11787.
29. Y.-F. Wang, Z.-R. Li, D. Wu, Y. Li, C.-C. Sun, F L. Gu, *J. Phys. Org. Chem,* **2017** , *30* , e3625.
30. F. Wahl, A. Weiler, P. Landenberger, E. Sackers, T. Voss, A. Haas, M. Lieb, D. Hunkler, J. Wörth, L. Knothe, H. Prinzbach, *Chem. Eur. J* , **2006** , *12* , 6255-6267.
31. J. Jia, H.-S. Wu, X.-H. Xu, X.-M. Zhang, H. Jiao, *J. Am. Chem. Soc* , **2008** , *130* , 3985-3988.
32. Y. Bai, Z.-J. Zhou, J.-J. Wang, Y. Li, D. Wu, W. Chen, Z.-R. Li, C.-C. Sun, *J. Phys. Chem. A* , **2013** , *117* , 2835-2843.
33. Z.-B. Liu, Y.-C. Li, J.-J. Wang, Y. Bai, D. Wu, Zhi-Ru Li, *J. Phys. Chem. A* , **2013** , *117* , 6678-6686.
34. N. Sadlej-Sosnowska, *Phys. Chem. Chem. Phys* , **2015** ,*17* , 23716-23719.

35. L. Zhang, S. Yan, R. I. Cukier, Y. Bu, *J. Phys. Chem. B* ,**2008** , *112* , 3767-3772.
36. P. Skurski, J. Simons, J. Chem. Phys, **2000** , *112* , 6563.
37. P. A. Limacher, K. V. Mikkelsen, H. P. Luthi, *J. Chem. Phys* ,**2009** , *130* , 194114.
38. J. E. Carpenter, F. Weinhold, *J Mol Struct: THEOCHEM* ,**1988** , *169* , 41-62.
39. K. Szalewicz and B. Jeziorski, *J. Chem. Phys* ., **1999** ,*109* , 1198.
40. Y. Zhao, D. G. Truhlar, *Theor. Chem. Acc* , **2008** ,*120* , 215-241.
41. B. Li, D. Peng, F. L. Gu, C. Zhu, *ChemistrySelect* ,**2018** , *3* , 12782-12790.
42. J. Hou, Y. Liu, X. Zhang, Q. Duan, D. Jiang, J. Qin, *New J. Chem* , **2018** , *42* , 1031-1036.
43. M. J. Frisch, G. W. Trucks, H. B. Schlegel, G. E. Scuseria, M. A. Robb, J. R. Cheeseman, J. A. Montgomery Jr., T. Vreven, K. N. Kudin, J. C. Burant, J. M. Millam, S. S. Iyengar, J. Tomasi, V. Barone, B. Mennucci, M. Cossi, G. Scalmani, N. Rega, G. A. Petersson, H. Nakatsuji, M. Hada, M. Ehara, K. Toyota, R. Fukuda, J. Hasegawa, M. Ishida, T. Nakajima, Y. Honda, O. Kitao, H. Nakai, M. Klene, X. Li, J. E. Knox, H. P. Hratchian, J. B. Cross, V. Bakken, C. Adamo, J. Jaramillo, R. Gomperts, R. E. Stratmann, O. Yazyev, A. J. Austin, R. Cammi, C. Pomelli, J. W. Ochterski, P. Y. Ayala, K. Morokuma, G. A. Voth, P. Salvador, J. J. Dannenberg, V. G. Zakrzewski, S. Dapprich, A. D. Daniels, M. C. Strain, O. Farkas, D. K. Malick, A. D. Rabuck, K. Raghavachari, J. B. Foresman, J. V. Ortiz, Q. Cui, A. G. Baboul, S. Clifford, J. Cioslowski, B. B. Stefanov, G. Liu, A. Liashenko, P. Piskorz, I. Komaromi, R. L. Martin, D. J. Fox, T. Keith, M. A. Al-Laham, C. Y. Peng, A. Nanayakkara, M. Challacombe, P. M. W. Gill, B. Johnson, W. Chen, M. W. Wong, C. Gonzalez, J. A. Pople, GAUSSIAN 09, revision A.02, Gaussian, Inc., Pittsburgh PA, **2009** .